Heliyon 10 (2024) e25602

Contents lists available at ScienceDirect

Heliyon

journal homepage: www.cell.com/heliyon

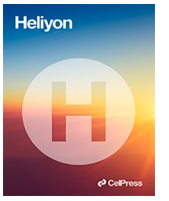

Research article

Electrochemical approach for the analysis of DNA degradation in native DNA and apoptotic cells

Lyubov E. Agafonova [a,*], Dmitry D. Zhdanov [a,b], Yulia A. Gladilina [a], Anastasia N. Shishparenok [a], Victoria V. Shumyantseva [a,c,**]

[a] Institute of Biomedical Chemistry, Pogodinskaya St. 10/8, 119121, Moscow, Russia
[b] Department of Biochemistry, Peoples' Friendship University of Russia Named After Patrice Lumumba (RUDN University), Miklukho-Maklaya St. 6, 117198, Moscow, Russia
[c] Department of Biochemistry, Pirogov Russian National Research Medical University, Ostrovitianova St. 1, 117997, Moscow, Russia

ARTICLE INFO

Keywords:
Bioelectrochemistry
Apoptosis
Plasmid DNA
Carbon nanotubes
Modified electrodes
DNA fragmentation

ABSTRACT

The aim of this work was to develop an electrochemical approach for the analysis of DNA degradation and fragmentation in apoptotic cells. DNA damage is considered one of the major causes of human diseases. We analyzed the cleavage processes of the circular plasmid pTagGFP2-N and calf thymus DNA, which were exposed to restriction endonucleases (the restriction endonucleases BstMC I and AluB I and the nonspecific endonuclease I). Genomic DNA from the leukemia K562 cell line was used as a marker of the early and late (mature) stages of apoptosis. Registration of direct electrochemical oxidation of nucleobases of DNA molecules subjected to restriction endonuclease or apoptosis processes was proposed for the detection of these biochemical events. Label-free differential pulse voltammetry (DPV) has been used to measure endonuclease activities and DNA damage using carbon nanotube-modified electrodes. The present DPV technique provides a promising platform for high-throughput screening of DNA hydrolases and for registering the efficiency of apoptotic processes. DPV comparative analysis of the circular plasmid pTagGFP2-N in its native supercoiled state and plasmids restricted to 4 and 23 parts revealed significant differences in their electrochemical behavior. Electrochemical analysis was fully confirmed by means of traditional methods of DNA analysis and registration of apoptotic process, such as gel electrophoresis and flow cytometry.

1. Introduction

Programmed cell death (apoptosis, autophagic death, and programmed necrosis) [1–3] has attracted the attention of numerous researchers for more than thirty years, primarily for two reasons. First, it plays an important role in morphogenetic processes and in the regulation of the cell count throughout the ontogenetic development of metazoan organisms. Second, the occurrence of many devastating diseases is associated with programmed cell death disorders, in which cells stop dying, tumors may develop, or death captures an excessive number of cells, which leads to pathological degeneration of tissues and organs.

One of the apoptotic markers is DNA fragmentation, which supports free 3' breaks and internucleosomal cleavage [4–6]. Patients

* Corresponding author.
** Corresponding author. Institute of Biomedical Chemistry, Pogodinskaya St. 10/8, 119121, Moscow, Russia.
E-mail addresses: agafonovaluba@mail.ru (L.E. Agafonova), Viktoria.shumyantseva@ibmc.msk.ru (V.V. Shumyantseva).

https://doi.org/10.1016/j.heliyon.2024.e25602
Received 2 October 2023; Received in revised form 30 January 2024; Accepted 30 January 2024
Available online 5 February 2024

with cancer exhibit altered fragmentation profiles of cell-free DNA (cfDNA) across the genome [7–9].

Timely monitoring of apoptosis can aid early diagnosis of diseases, scrutiny of the effectiveness of medicinal preparations, and development of new drugs [4]. Different types of sensor systems, such as electron microscopy or fluorescence microscopy, are used for the early diagnosis of programmed cell death and play a very important role in preventing disease progression, such as cancer, aging, and neurological diseases [10,11].

There are a number of effective methods for discriminating between living and dead cells. These methods include fluorescent techniques with double staining for the analysis of cell survival and cell cycle monitoring for the detection of apoptosis via the binding of annexin V [6]. Laboratory methods for analyzing the functional state of cells (assessment of the rate and degree of “spreading" of cells in adhesive cultures, assessment of mitochondrial potential and evaluation of the redox potential of cells) are also used [10].

Electrochemical methods in biochemical and biomedical research are based on the registration of processes during the acquisition or release of electrons by biological molecules. Currently, electrochemical methods are being actively developed and have a number of advantages, such as multiparametric analysis (potential, current intensity, area under the signal), quantitative determination of the electroactive biocomponent and determination of its properties based on the application of the fundamental laws of electrochemistry. Label-free analysis does not require additional expensive reagents. In addition, it is possible to use various types of electrodes, disposable or reusable interchangeable electrodes obtained by screen printing; measuring devices with software can be stationary and portable.

Electrochemical techniques are widely used to detect DNA damage and fragmentation [11,12]. The most frequently used approach is the registration of 8-oxo-guanine formation during oxidative DNA damage [13]. Indirect methods based on the registration of electron transfer processes in the presence of mediators, for example, $[Os(bpy)_2(PVP)10Cl]^+$ and $[Ru(bpy)_2(PVP)10Cl]^+$ metallopolymers (by electrochemistry for electroactive Os^{3+}/Os^{2+} and $Ru^{3+/}Ru^{2+}$ centers) [11] or $[Fe(CN)_6]^{4-}/^{3-}$ anions, indicate changes in the state of the DNA layer on the electrode surface on the basis of electrostatic repulsion between the indicator anion and the negatively charged DNA backbone [12]. The heterocyclic bases of nucleic acids possess intrinsic electrochemical activity [12,14]. Changes in the intensities of the oxidative peak current of nucleic bases can also be employed for the detection of DNA lesions [11].

For cell death to be classified as an apoptotic process, nuclear condensation and fragmentation, cleavage of chromosomal DNA into internucleosomal fragments and packaging of the deceased cell into apoptotic bodies without plasma membrane breakdown must be observed [2]. DNA length change (DNA fragmentation) is a recognized marker of programmed cell death [15], and the development of approaches for the analysis of DNA degradation is a relevant objective.

The existing methods for registering DNA/RNA using electron transfer mediators or nucleic acid labels (enzymes and/or conductive polymers, nanoparticles in the form of quantum dots or transition metal complexes, and electroactive dyes) are highly sensitive but do not allow direct registration of purine and/or pyrimidine bases [16–18]. Label-free electrochemical oxidation of nucleotides, oligonucleotides and DNA/RNA nucleobases is a suitable platform for direct registration of polymeric macromolecules and biochemical processes involving these biomaterials bearing hereditary information [9,16].

For sensitive detection of DNA damage, techniques involving enzymatic processing of damaged DNA are used. These enzymes include N-glycosylases (for removing damaged nucleobases), endonucleases (for introducing strand breaks), exonucleases (for removing part of the DNA strand next to the lesion), polymerases (for resynthesizing the exonuclease-digested segment) and ligases (for finishing the repair process by SSB sealing) [12]. The enzymatic digestion of DNA with the DNA repair enzyme exonuclease III (exoIII), followed by single-strand (ss) selective DNA modification by a complex of osmium tetroxide with 2,2′-bipyridine, was monitored [19]. Damaged DNA digested by exonuclease III (EXOIII) was detected by CV via electrocatalytic oxidation of guanine residues by a ruthenium bipyridine complex [20].

In this study, we propose for the first time the DPV method for direct registration of fragmentation and cleavage (degradation) induced by restriction endonucleases (restriction endonucleases BstMC I and AluB I and nonspecific endonuclease I). Our approach involved the use of various DNA forms, such as the circular plasmid pTagGFP2-N, low-molecular-weight dsDNA from herring sperm, high-molecular-weight calf thymus DNA and genomic DNA isolated from the human chronic myelogenous leukemia K562 cell line. Analysis of DNA degradation and fragmentation in apoptotic cells at the early and late stages of cell death was also performed with high sensitivity. As a sensing element of our assay, we used screen-printed electrodes modified with carbon nanotubes. The novelty of our approach lies in the registration of real sample detection subjected to enzymatic digestion or impact.

2. Materials and Methods

2.1. Reagents and electrochemical equipment

Water dispersions of 0.4 % single-wall carbon nanotubes (SWCNTs; diameter, 1.6 ± 0.4 nm; length, >5 μM; surface area, 1000 m^2/g) of TUBALL™ BATT H_2O stabilized with carboxymethylcellulose were obtained from OCSIAL Ltd. (https://ocsial.com). Potassium phosphate monobasic (≥99 %) and potassium phosphate dibasic trihydrate (≥99 %) were purchased from Sigma–Aldrich. Sodium chloride (99.5 %) was purchased from Acros Organics.

Fish-sperm double-stranded DNA (dsDNA) from herring sperm as a lyophilized powder was obtained from Sigma–Aldrich (D 3159). The plasmid pTagGFP2-N vector (#FP192) was obtained from Evrogen (Moscow, Russia). Calf thymus DNA was obtained from Serva (Heidelberg, Germany).

All the other chemicals used were of analytical grade and used without further purification. All aqueous solutions were prepared using Milli-Q water (18.2 MΩcm) purified with a Milli-Q water purification system by Millipore.

Screen-printed electrodes (SPEs) with a working area of 0.0314 cm^2, auxiliary graphite electrodes and a silver/silver chloride

reference electrode (Ag/AgCl) were obtained from ColorElectronics, Russia (http://www.colorel.ru). All potentials refer to the Ag/AgCl reference electrode.

Electrochemical studies (differential pulse voltammetry [DPV]) were performed using a PalmSens potentiostat (PalmSens BV, the Netherlands) with PSTrace software (version 5.8) in 0.1 M potassium phosphate buffer with 50 mM NaCl as the supporting electrolyte (PBS, pH 7.4). All the electrochemical experiments were carried out using a Faraday cage (Metrohm Autolab BV, Netherlands) at room temperature (25 ± 3 °C) in a 60 μL drop of PBS placed onto the SPE to cover the surface of all three electrodes. The DPV method was used with the following parameters: potential range of (0.2–1.2) V, pulse amplitude of 0.025 V, potential step of 0.005 V, pulse duration of 0.05 s, and scan rate of 0.05 V/s. All the electrochemical experiments were performed in triplicate, and the quantitative characteristics (maximum amplitude of peak current, peak potential and peak area) of the oxidation peaks were within 10 % (the standard deviation, SD ≈ 10 %), which highlights the inherent repeatability of the electrochemical setup. All the voltammograms were baseline-corrected using the moving average with a step window of 5 mV included in PSTrace (version 5.8) software.

The raw DPV data were analyzed using derivative calculations in PSTrace software (version 5.8) to increase the sensitivity of the DPV analysis.

2.2. Electrode modification

The working electrodes were modified by 2 μL of a preliminary 5-fold dilution in a distilled water dispersion of SWCNT TUBALL™ BATT H_2O (0.75 ± 0.05 mg/mL). The SPE/SWCNT electrodes were kept at room temperature until they were completely dry (~25 min). Modified electrodes were pretreated in PBS, pH 7.4, by DPV three times. Two microliters of the probe was dropped onto the surface of the modified electrode and incubated for 24 h at +4 °C before the measurements. A 60 μL drop of PBS was placed on the SPE to cover the surface of all three electrodes and horizontal measurement regimen was used for all the experiments.

2.3. Plasmid propagation and restriction

The vector pTagGFP2-N (4.7 kb) was transformed into the *Escherichia coli* XL1 strain, after which the cells were cultivated in LB Broth, Miller (LB) medium (VWR Chemicals, Solon, OH) for 16 h in the presence of 30 μg/mL kanamycin (Paneco, Moscow, Russia). The plasmid was purified using the Plasmid Miniprep Kit (Evrogen, Moscow, Russia). The restriction endonucleases BstMC I (SE-E071) and AluB I (SE-E549), the nonspecific endonuclease I (SE-E323) and the molecular weight marker 100 bp+1.5 Kb+3 Kb (SE-M27) were obtained from SibEnzyme (Novosibirsk, Russia).

One milligram of plasmid DNA was subjected to specific restriction for four parts by the restriction endonuclease BstMC I or for 23 parts by AluB I according to the manufacturer's recommendations. The restriction map for the enzymes used is shown in Scheme 1S (Supplementary data). Nonspecific digestion of plasmid or genomic DNA from calf thymus (1 mg) was performed using Endonuclease I according to the manufacturer's recommendations. The digested DNA fragments were purified with a Cleanup S-Cap Kit for DNA purification from reaction mixtures (Evrogen, Moscow, Russia) using phosphate-buffered saline (PBS, NaCl 137 mM; KCl 2.7 mM; Na_2HPO_4 10 mM; KH_2PO_4 1.8 mM; pH 7.4). The DNA yield was measured by a multimodal reader SuPerMax 3100 (Flash Spectrum, Shanghai, China), and the concentrations were equilibrated for each sample. Visualization of the restricted or digested fragments was performed via 1.5 % agarose gel electrophoresis and TBE electrophoresis buffer (0.1 M Tris base, boric acid; 0.1 M; 0.002 M EDTA (disodium salt); pH 8.0). Ten microliters of sample was added to each well of the gel comb. The gels were stained with ethidium bromide and photographed under UV light in a ChemiDoc™ XRS imaging system (Bio-Rad, Hercules, CA).

2.4. Cell cultivation and induction of apoptosis

The human chronic myelogenous leukemia K562 cell line (ATCC, Manassas, VA) was grown in RPMI-1640 medium (Paneco, Moscow, Russia) supplemented with 5 % fetal bovine serum (Capricorn Scientific, Ebsdorfergrund, Germany) and 1 % sodium pyruvate (Paneco, Moscow, Russia). The cells were grown in 5 % CO_2/95 % air in a humidified atmosphere at 37 °C. To induce apoptosis, L-asparaginase *Erwinia carotovora* (IBMC, Moscow, Russia [21]) was added to growing cells at a concentration of 20 U/ml, and the cells were incubated for 60 or 72 h. To measure apoptosis, the cells were dissociated using trypsin, resuspended in PBS and incubated with Annexin V-FITC and propidium iodide (PI) from a FITC Annexin V/Dead Cell Apoptosis Kit (Life Technologies, Carlsbad, CA) according to the manufacturer's protocol. The counting of $5x10^4$ cells at each point was performed by flow cytometry with a MACS Quant Analyzer 10 (Miltenyi Biotec, Bergisch Gladbach, Germany) as we previously described [22]. The number of cells with damaged DNA was determined by terminal deoxynucleotidyl transferase-mediated d-UTP nick end labeling (TUNEL assay) [23] using a Click-iT Plus TUNEL assay (Thermo Fisher Scientific, Inc., Waltham, MA) according to the manufacturer's protocol. Genomic DNA was isolated from cells via a DNA isolation kit for the isolation of genomic DNA from cells, tissues, and blood (DU-250, Biolabmix, Novosibirsk, Russia). Isolated DNA was visualized as described above. Statistical analysis involving Student's t–test was implemented with statistical software (version 9.0; StatSoft, Tulsa, OK). Differences described by $p \leq 0.05$ were considered significant. The results are presented as the mean ± standard error of the mean (SEM).

3. Results and discussion

3.1. Electrochemical characteristics of the plasmid pTagGFP2-N

Scree-printed electrodes (SPEs) are widely used in the electrochemical sensing of biomolecules, such as heme proteins, drugs, and DNA; for drug-protein interactions; and for drug-DNA interactions [24–26]. Carbon nanomaterials significantly improve the sensitivity of electrodes [27]. In our previous papers, we described in detail the electrochemical characteristics and behavior of SPEs modified by means of dispersion of SWCNTs in carboxymethylcellulose (SPE/SWCNT) [28–30].

In our investigation, we used a DNA plasmid with a size of 4729 bp. To study the electrochemical profile of the plasmid pTagGFP2-N in the native state at a concentration of 0.1 mg/mL, differential pulse voltammetry (DPV) was performed on the SPE/SWCNT/plasmid pTagGFP2-N. Earlier, we showed that the DPV technique using SPE/SWCNTs allows us to detect the direct electrochemical oxidation of the purine heterocyclic bases guanine (G) and adenine (A) of total DNA isolated from transfected and control SkBr-3 cells [29], as well as the oxidation of guanine (G), adenine (A) and the thymine pyrimidine base (T), as shown for dsDNA from herring sperm [30–34]. For the supercoiled plasmid pTagGFP2-N, as shown in Fig. 1, one broad peak was observed with a peak potential centered at $E = 0.50 \pm 0.01$ V, corresponding to the possible overlapping electrochemical oxidation of G and A nucleobases for the plasmid pTagGFP2-N DNA at a concentration of 0.1 mg/mL.

A comparison of the DPV results of dsDNA from herring sperm at the same concentration of 0.1 mg/mL revealed the electrochemical oxidation of three heterocyclic bases, G, A, and T, registered at peak potentials of $E(G) = 0.49 \pm 0.01$ V; $E(A) = 0.84 \pm 0.01$ V; and $E(T) = 1.11 \pm 0.01$ V, respectively. For an SPE/SWCNT blank electrode without DNA, no peaks were observed during potential scanning (Fig. 1, dashed line). The registration of three heterocyclic bases, G, A, and T, for partially fragmented dsDNA from herring sperm (MW ~10 ÷ 30 kDa) may be associated with greater availability of G, A, and T for the electrooxidation reaction on the electrode in comparison with supercoiled circular plasmid DNA, with a molar mass of 1,891,600 Da according to sequence data (Supplementary data, Scheme 1S). Our results are in accordance with earlier published data on the electroanalysis of supercoiled (scpUC19) and linear (pUC19) plasmids [35,36] and the electroanalysis of dsDNA [16,17,30–34,36,37]. Supercoiled circular plasmid DNA (scpUC19) or linear plasmid can be registered electrochemically with overlapping oxidation of heterocyclic nucleic bases (G and A, presumably) in the broad range of potentials on glassy carbon electrodes using 0.25 M acetate buffer with 18 mM $MgCl_2$, pH 4.7 [35,36]. In contrast, dsDNA can be registered as two or three separate peaks corresponding to G, A, and T electrochemical oxidation [16,17,30–34,36,37].

3.2. Comparative electrochemical characteristics of native and restricted circular plasmid DNAs

Nucleases, which are hydrolases, are capable of cleaving DNA into oligonucleotide fragments of different lengths. The cleavage of DNA by endonucleases or exonucleases plays a fundamental role in replication, recombination, DNA repair, molecular cloning, and genotyping [38]. Different methods, such as polyacrylamide gel electrophoresis, radioactive labeling, resonance energy transfer, high-performance liquid chromatography (HPLC), colorimetric sensors, fluorescent sensors and enzyme-linked immunosorbent assays (ELISAs), are commonly used for nuclease assays [38]. However, these methods are time-consuming and require complicated sample preparations with additional reagent sets. Electrochemical label-free sensors based on direct analysis of heterocyclic bases have advantages such as rapid response and analysis of pyrimidine and purine bases registered at nonoverlapping potentials [16,17,30–34,36,37].

In our study of targeted DNA fragmentation/restriction, we analyzed aqueous samples of plasmid DNA and digested (fragmented) DNA previously purified from restriction enzymes and buffers. Comparative analysis of the plasmid restricted to 4 parts with the plasmid in its native supercoiled state at concentrations of 0.067–0.1 mg/mL showed significant differences in their electrochemical

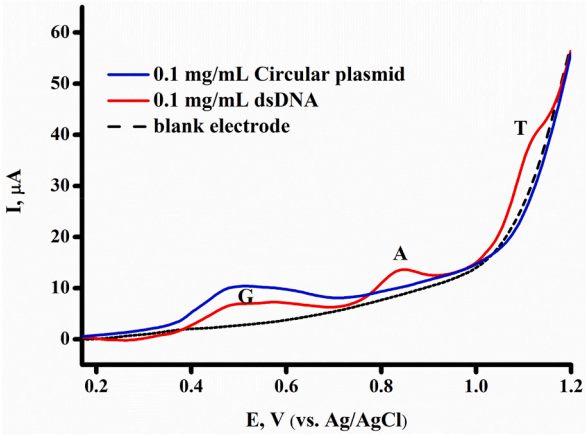

Fig. 1. DPVs for SPE/SWCNT in the absence (dashed line, blank electrode) or presence (red line) of dsDNA from herring sperm and (blue line) plasmid DNA at a concentration of 0.1 mg/mL.

signatures, as determined with DPV techniques. The DP voltammograms of the circular plasmid demonstrated only one peak centered at E = 0.50 ± 0.01 V. The DP voltammogram obtained by digestion (fragmented) into the 4-part plasmid exhibited two well-defined anodic peaks at E_1 = 0.50 ± 0.01 V and E_2 = 0.70 ± 0.01 V (Fig. 2), with comparable peak intensities.

The concentration dependencies of the peak current intensities were registered for 0.067 mg/mL and 0.050 mg/mL of the plasmid DNA restricted into 4 fragments. However, at a concentration of 0.050 mg/mL, only one pronounced oxidation peak was recorded at E = 0.50 ± 0.01 V (Fig. 3).

At a concentration of 10 ng/μL (0.01 mg/mL), the peak currents were 5.66 ± 0.58 μA and 5.67 ± 0.18 μA at a peak potential of E = 0.50 ± 0.01 V, which was consistent within the measurement error for the circular plasmid and plasmid restricted into 4 fragments, respectively (Fig. 4A). The first derivative of the peak current (I) vs. peak potential (E) curves of the DPV responses could improve the signal-to-noise ratio (Fig. 4B).

For a plasmid restricted into 23 fragments at a concentration of 10 ng/μL, the DP voltammogram ("electrochemical signature") demonstrated a resolved oxidation curve with two peaks, which is shown in Fig. 4B on differential curves, and an increase in the electrooxidation peak current of 16 % was observed at a peak potential of E = 0.50 ± 0.01 V (Fig. 4C). It is possible to assume, based on our experimental data, that with increased DNA fragmentation (Fig. 4D), the number of registered signals (peaks corresponding to the oxidation of heterocyclic bases) and the intensity of the peak currents of oxidation signals increase.

A possible explanation for these experimental data is the accessibility of DNA purine bases for electrochemical oxidation on the electrode surface. In the case of circular plasmid DNA, heterocyclic bases were embedded within the more compact circular plasmid structure and less exposed to the electrode surface, reflecting lower peak current intensities. Fragmentation of 23 parts facilitates the oxidation of heterocyclic bases due to increased availability of damaged DNA for electrons. It is also possible to assume that, in fragments of different lengths, different exposed populations of G and A residues are present (Supplementary data, Table 1S).

The quantitative characteristics of the measured samples of circular plasmid DNA or plasmid DNA restricted to 4 or 23 fragments and restriction sites are given in the appendix in Table 2S and Scheme 1S (Supplementary data).

3.3. Electrochemical characteristics of nonspecifically digested plasmid DNA and calf thymus DNA

As shown in Fig. 1, the electrochemical signature of the circular plasmid at a concentration of 0.1 mg/mL demonstrated only one peak centered at E = 0.50 ± 0.01 V. The native calf thymus DNA exhibited two well-defined anodic peaks at E(G) = 0.49 ± 0.01 V and E(A) = 0.83 ± 0.01 V (Fig. 5).

For nonspecifically digested plasmid DNA and calf thymus DNA to form low-molecular-weight fragments (Fig. 6), the DNA was exposed to endonuclease I, which allowed us to obtain 3–70-mer fragments (Fig. 6C). For the electrochemical registration of the DP signatures of the digested plasmid DNA and calf thymus DNA, we used the sample−control subtraction method to take into account the side effects of the voltammograms of the restrictive medium with endonuclease.

As shown in Fig. 6, the signatures of damaged (degraded) plasmid DNA (Fig. 6A, red line) and calf thymus DNA (Fig. 6B, red line) demonstrated a complicated DPV profile corresponding to DNA with restrictive medium and endonuclease. To visualize the voltammograms of the degraded plasmid DNA and calf thymus DNA (Fig. 6A and B, blue lines, respectively), we subtracted the DP voltammograms of the restriction medium with endonuclease I (Fig. 6A and B, black line) from the DVPs of the degraded plasmid DNA and calf thymus DNA (Fig. 6A and B, red line). As shown in Fig. 6A and B (blue lines), the DPVs of degraded plasmid DNA and calf thymus DNA themselves exhibited two peaks that were shifted in the positive direction in comparison with those of dsDNA [31], which indicates the difficulty of electrooxidation of G and A on the electrode surface due to the influence of the restrictive medium during the oxidation processes.

The quantitative characteristics of the degraded plasmid DNA are given in the appendix in Table 2S (Supplementary data).

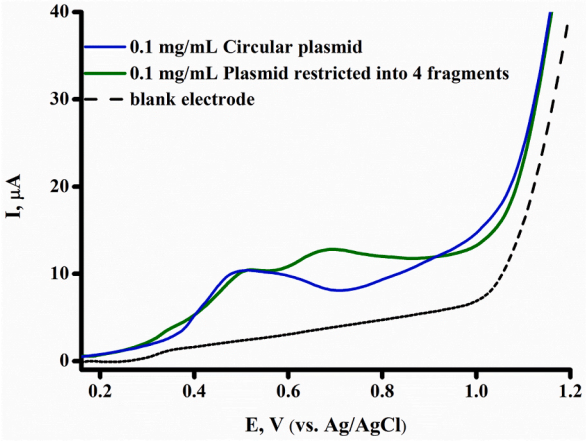

Fig. 2. DPVs of the SPE/SWCNTs in the presence (blue line) of the plasmid DNA and (green line) of the plasmid DNA restricted to 4 fragments at a concentration of 0.1 mg/mL in the absence of a DNA blank electrode (dashed line).

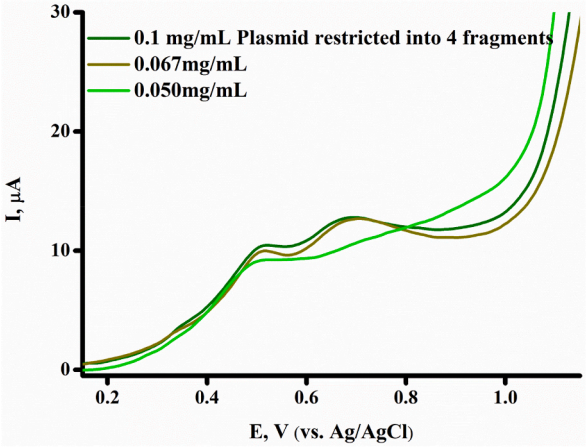

Fig. 3. DPVs for the SPE/SWCNT/plasmid DNA restricted into four fragments at different concentrations (0.05–0.1) mg/mL.

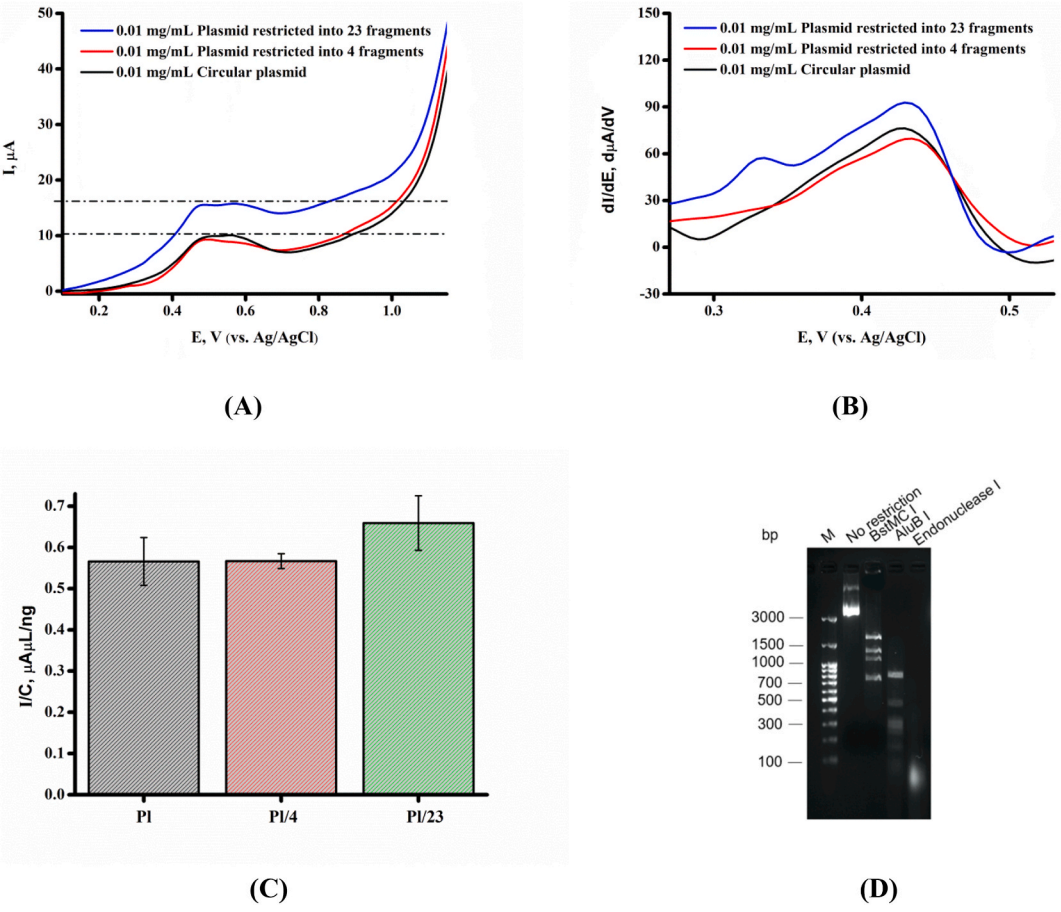

Fig. 4. **(A)** DPVs for the SPE/SWCNT/circular plasmid DNA and plasmid DNA restricted to 4 or 23 fragments at a concentration of 0.01 mg/mL; **(B)** Derivatives dI/dE of signals for the SPE/SWCNT/circular plasmid DNA or circular plasmid DNA restricted to 4 or 23 fragments; **(C)** Histograms corresponding to the ratio of the I/C signals for circular plasmid DNA (Pl) or plasmid DNA restricted to 4 (Pl/4) and 23 (Pl/23) fragments at a concentration of 0.01 mg/mL; **(D)** Agarose gel electrophoresis of pTagGFP2-N subjected to restriction with the specific nucleases BstMC I or AluB I or nonspecific endonuclease I. *Original agarose gel image is shown in Fig. 1S in the supplementary file.*

Table 1
The electrochemical characteristics of DNA degradation in apoptotic cells, measured for SPE/SWCNT electrode modification in PBS (pH = 7.4).

[Sample DNA]/0.55 mg/mL		Quantitative characteristics (maximum amplitude of peak current, I_{ox}/μA, and peak area, Peak area/μAV) of oxidation peaks at the appropriate potentials (E_{ox}/V)		
	E_{ox}	0.49 ± 0.01	0.84 ± 0.01	1.11 ± 0.01
[Intact DNA from cells]	I_{ox}	4.64 ± 0.45	1.92 ± 0.10	1.87 ± 0.19
	Peak area	0.98 ± 0.10	0.171 ± 0.014	0.087 ± 0.009
[Native calf thymus DNA]	I_{ox}	4.28 ± 0.40	0.483 ± 0.007	–
	Peak area	0.931 ± 0.092	0.037 ± 0.002	
[DNA degradation at early apoptosis in cells]	I_{ox}	3.87 ± 0.39	2.452 ± 0.082	3.173 ± 0.093
	Peak area	0.81 ± 0.09	0.228 ± 0.004	0.169 ± 0.010
[DNA degradation at later apoptosis in cells]	I_{ox}	3.69 ± 0.38	3.57 ± 0.36	5.54 ± 0.36
	Peak area	0.786 ± 0.080	0.349 ± 0.036	0.327 ± 0.023

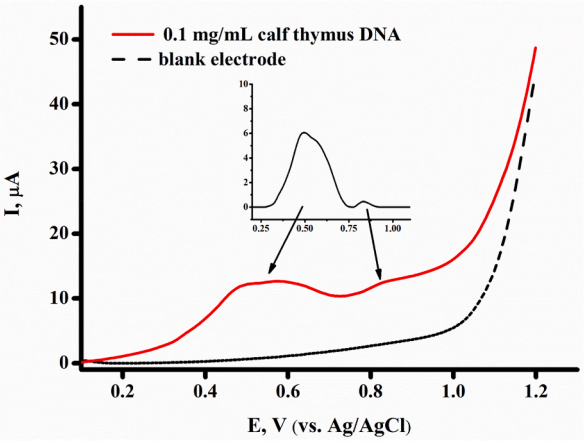

Fig. 5. DPVs for SPE/SWCNTs in the absence (dashed line, blank electrode) and presence (red line) of native calf thymus DNA at a concentration of 0.1 mg/mL.

3.4. Analysis of DNA degradation in apoptotic cells

The registration of the early stages of apoptosis requires reliable methods involving the use of programmed cell death-specific markers and real-time monitoring of death kinetics [4]. DNA fragmentation is initiated at the late stages of apoptosis by apoptotic endonucleases, ensuring the irreversibility of cell death [39,40].

In our investigation, we used DPV profiling of genomic DNA from apoptotic cells. Genomic DNA was isolated from the human chronic myelogenous leukemia K562 cell line as described in the Materials and Methods. Analysis of DNA isolated from cells was carried out in the potential range of 0 to +1.2 V by DPV using SPE/SWCNT-modified electrodes. The DP voltammogram for intact DNA isolated from cells revealed three peaks at potentials of E(G) = 0.49 ± 0.01 V, E(A) = 0.84 ± 0.01 V, and E(T) = 1.12 ± 0.01 V (Fig. 7, orange line). A comparison of DPV profiles for intact DNA isolated from cells and native calf thymus DNA at a concentration of 0.55 mg/mL is shown in Fig. 7. As shown in Fig. 7, native calf thymus DNA exhibited a broad peak at +0.4 ÷+0.7 V and an additional peak at +0.84 V in comparison with intact DNA isolated from cells. These differences may be related to the molecular mass and tertiary structure of the DNA under study.

To induce apoptosis, we used the L-asparaginase *Erwinia carotovora*, whose proapoptotic activity is not associated with direct action on cellular DNA [41]. Asparaginase-sensitive K562 cells were incubated for 60 or 72 h, after which the induction of apoptosis was monitored via flow cytometry (Fig. 8). DNA fragmentation was detected by TUNEL assay and visualized by gel electrophoresis. We demonstrated that after incubating with L-asparaginase for 60 h, most of the cells were in the early stage of apoptosis (Fig. 8A and B), which was associated with an increased proportion of Annexin-V-positive cells. At 72 h, most of the cells were in the late apoptosis stage, which was determined by an increased proportion of both Annexin-V- and PI-positive cells. The development of apoptosis was associated with the rate of DNA degradation: 42.1 ± 4.63 % of cells were TUNEL-positive after 60 h of incubation (Fig. 8 C and D), and 68.31 ± 5.27 % were TUNEL-positive after 72 h. DNA degradation was also confirmed by agarose gel electrophoresis (Fig. 8 E).

In our study, we performed direct electrochemical analysis of DNA degradation in apoptotic cells. There was a clear difference in the DP voltammograms ("electrochemical profiles") of DNA during early and late apoptosis. As shown in Fig. 9A and Table 1, three peaks corresponding to the electrochemical oxidation of G, A and T heterocyclic residues were observed at peak potentials of E(G) = 0.49 ± 0.01 V; E(A) = 0.84 ± 0.01 V; and E(T) = 1.11 ± 0.01 V, respectively.

The broad and undulating peak centered at E = 0.49 ± 0.01 V represents overlapping signals of heterocyclic nucleobases

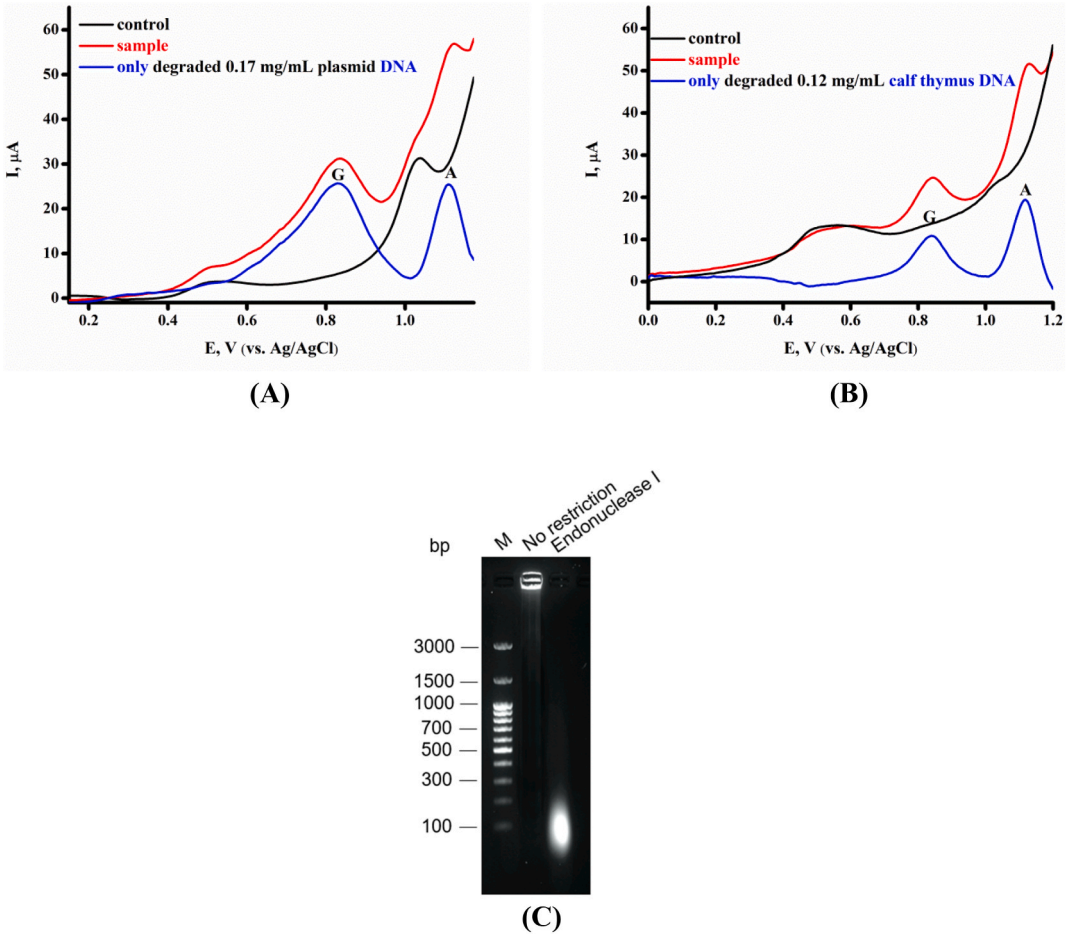

Fig. 6. DPVs for SPE/SWCNTs in the presence of **(A)** plasmid DNA and **(B)** calf thymus DNA. The sample is restrictive medium with endonuclease I and DNA (red lines), the control is restrictive medium with endonuclease without DNA (black line), and the blue lines represent only the degraded plasmid and calf thymus DNA as the difference between sample and control. The plasmid DNA and calf thymus DNA concentrations were 0.17 and 0.12 mg/mL, respectively. **(C)** Agarose gel electrophoresis of calf thymus DNA subjected to restriction with nonspecific endonuclease I. *Original agarose gel image is shown in Fig. 1S in the supplementary file.*

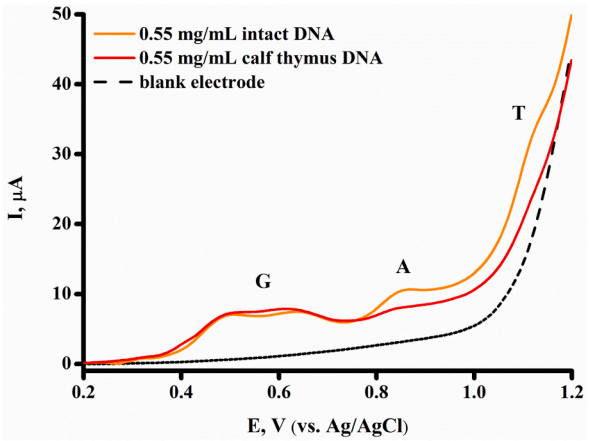

Fig. 7. DPV profiles for SPE/SWCNTs in the absence (dashed line, blank electrode) or presence (red line) of native calf thymus DNA and (orange line) of intact DNA at a concentration of 0.55 mg/mL.

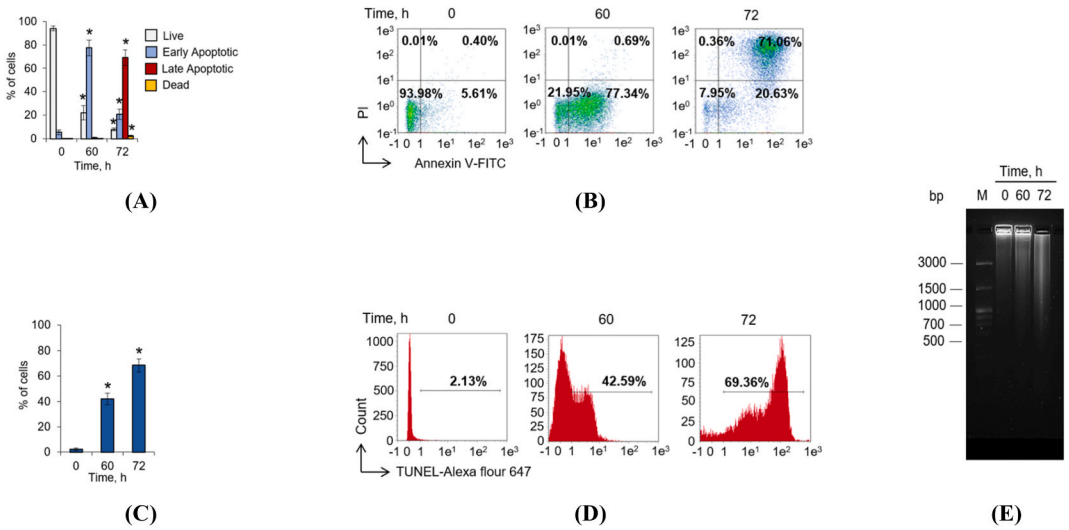

Fig. 8. Detection of cell apoptosis and DNA degradation in apoptotic cells K562 cells were incubated with L-asparaginase for 60 or 72 h. **(A)** Histograms of live, apoptotic and dead cells. **(B)** Representative flow cytometry plots for cells labeled with annexin V–FITC and PI. The ratios of living cells (lower left quadrants), early apoptotic cells (lower right quadrants), late apoptotic cells (upper right quadrants) and dead cells (upper left quadrants) are presented. **(C)** Histograms showing an increasing number of TUNEL-positive cells, indicating an increase in the percentage of cells with degraded DNA after apoptosis induction. **(D)** Representative TUNEL assay flow cytometry plots for incubated cells. **(E)** Agarose gel electrophoresis of DNA isolated from control cells or cells after apoptosis induction. The results are presented as the mean ± standard error of the mean (SEM); *p ≤ 0.05 vs. control untreated cells according to Student's t–test; n = 4. *Original agarose gel image is shown in Fig. 2S in the supplementary file.*

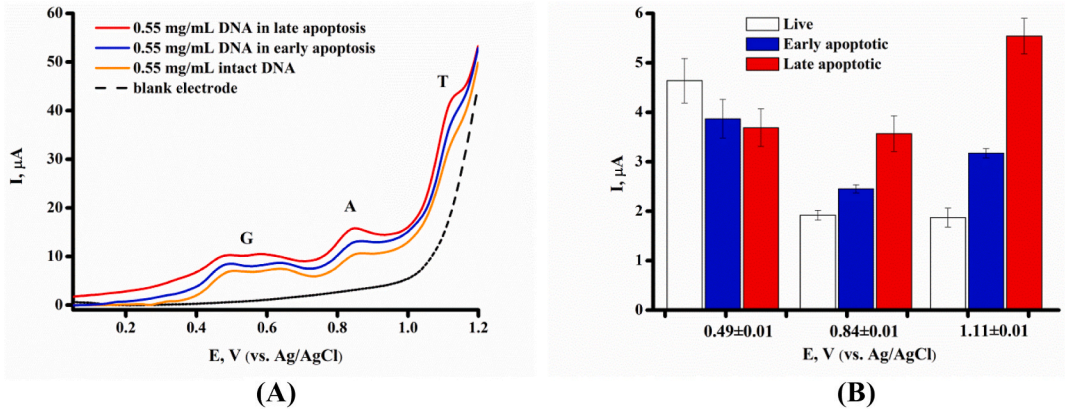

Fig. 9. Detection of degraded DNA from apoptotic cells via an electrochemical method **(A)** DPV profiles for SPE/SWCNTs in the absence (dashed line, blank electrode) or presence (red line) of DNA during late apoptosis (blue line) of DNA during early apoptosis and (orange line) of intact DNA at a concentration of 0.55 mg/mL; **(B)** histograms corresponding to the ratio of the DNA electrooxidation signals at a concentration of 0.55 mg/mL in apoptotic cells at different stages of cell death.

electrochemical oxidation in fragments of different lengths depending on the percentage of apoptotic cells. With an increase in the percentage of cell apoptosis, the electrooxidation of A and T heterocyclic residues of DNA increased (Fig. 9B and Table 1).

DP voltammograms ("electrochemical profile") of DNA degradation in apoptotic cells may be explained by the greater availability of G, A, and T for electrochemical oxidation on the electrode.

4. Conclusion

DNA is the main participant in the genome in living cells. The main feature of DNA is susceptibility to fragmentation, degradation or damage, as well as pathological processes and apoptosis induced by endogenous or exogenous factors. Robust and sensitive detection methods for detecting DNA fragmentation and cleavage are urgently needed.

An electrochemical method for registering target fragments of the high-molecular-weight plasmid pTagGFP2-N was proposed by means of DPV via the modification of screen-printed electrodes with SWCNTs. The electrochemical DP voltammograms of the circular

plasmid revealed one broad overlapping peak in the region of electrochemical oxidation of heterocyclic bases at a potential of E = +0.50 ± 0.01 V. When the plasmid was fragmented into four parts using the specific restriction enzyme BstMC I, two peaks corresponding to the electrooxidation of heterocyclic bases at potentials of E_1 = +0.50 ± 0.01 V and E_2 = +0.70 ± 0.01 V were observed. Fragmentation of the circular plasmid pTagGFP2-N into 23 parts with the restriction endonuclease AluB I also results in a more pronounced electrochemical oxidation peak current, corresponding to oxidation of heterocyclic bases. DPV of the circular plasmid pTagGFP2-N fragmented into 23 parts allowed registering the appearance of two peaks (probably guanine and adenine), as revealed by differentiated DP voltammograms. Total degradation of the plasmid pTagGFP2-N with nonspecific endonuclease I resulted in more pronounced anodic electrochemical oxidation signals corresponding to nucleobases of DNA, which were shifted to the positive potential region compared to those of the circular plasmid and partially fragmented samples. This potential shift is typical for native dsDNA, oligonucleotides and components of nucleic acids (nucleotides, nucleosides and heterocyclic bases). Based on our experimental data, we can conclude that with an increase in the number of fragments of DNA damage (fragmentation), (i) the number of registered peaks corresponding to the electrooxidation of heterocyclic bases increases, and (ii) the intensity of the peak current of electrooxidation signals increases. Thus, electroanalysis is a method of choice for monitoring the fragmentation and degradation of a supercoiled circular plasmid with high sensitivity (up to 10 ng/μL). The use of DNA fragmentation as an apoptosis marker allows early and late apoptosis to be monitored in mammalian cells.

CRediT authorship contribution statement

Lyubov E. Agafonova: Writing – review & editing, Writing – original draft, Methodology, Investigation. **Dmitry D. Zhdanov:** Writing – review & editing, Investigation, Formal analysis, Data curation. **Yulia A. Gladilina:** Investigation, Formal analysis. **Anastasia N. Shishparenok:** Investigation, Formal analysis. **Victoria V. Shumyantseva:** Writing – review & editing, Methodology, Data curation, Conceptualization.

Declaration of competing interest

The authors declare that they have no known competing financial interests or personal relationships that could have appeared to influence the work reported in this paper.

Acknowledgements

This work was financed by the Ministry of Science and Higher Education of the Russian Federation within the framework of state support for the creation and development of World-Class Research Centers ‘Digital Biodesign and Personalized Healthcare’ (No 075-15-2022-305).

Appendix A. Supplementary data

Supplementary data to this article can be found online at https://doi.org/10.1016/j.heliyon.2024.e25602.

References

[1] E. Ogier-Denis, P. Codogno, Autophagy: a barrier or an adaptive response to cancer, Biochim. Biophys. Acta 1603 (2003) 113–128, 10.1016/S0304-419X(03)00004-0.
[2] A.L. Edinger, C.B. Thompson, Death by design: apoptosis, necrosis and autophagy, Curr. Opin. Cell Biol. 16 (2004) 663–669, 10.1016/j.ceb.2004.09.011.
[3] N.N. Danial, S.J. Korsmeyer, Cell death critical control points, Cell 116 (2004) 205–219, 10.1016/S0092-8674(04)00046-7.
[4] R. Akçapınar, B. Garipcan, V. Goodarzi, L. Uzun, Designing of various biosensor devices for determination of apoptosis: a comprehensive review, Biochem. Biophys. Res. Commun. 578 (2021) 42–62, 10.1016/j.bbrc.2021.08.089.
[5] G. Ichim, S.W. Tait, A fate worse than death: apoptosis as an oncogenic process, Nat. Rev. Cancer 16 (2016) 539–548, 10.1038/nrc.2016.58.
[6] J. Yin, P. Miao, Apoptosis evaluation by electrochemical techniques, Chem. Asian J. 11 (2016) 632–641, 10.1002/asia.201501045.
[7] S. Cristiano, A. Leal, J. Phallen, J. Fiksel, V. Adleff, D.C. Bruhm, S.Ø. Jensen, J.E. Medina, C. Hruban, J.R. White, D.N. Palsgrove, N. Niknafs, V. Anagnostou, P. Forde, J. Naidoo, K. Marrone, J. Brahmer, B.D. Woodward, H. Husain, K.L. van Rooijen, V.E. Velculescu, Genome-wide cell-free DNA fragmentation in patients with cancer, Nature 570 (2019) 385–389, 10.1038/s41586-019-1272-6.
[8] A. Campos-Carrillo, J.N. Weitzel, P. Sahoo, R. Rockne, J.V. Mokhnatkin, M. Murtaza, S.W. Gray, L. Goetz, A. Goel, N. Schork, T.P. Slavin, Circulating tumor DNA as an early cancer detection tool, Pharmacol. Therapeut. 207 (2020) 107458, 10.1016/j.pharmthera.2019.107458.
[9] M. Augustín, R. Pfeifer, J. Barek, V. Vyskočil, Comparison of two pyrolytic graphite representatives in the construction of hybrid electrochemical DNA biosensors for monitoring DNA damage, J. Electroanal. Chem. 908 (2022) 116095, 10.1016/j.jelechem.2022.116095.
[10] M. Hasanzadeh, N. Shadjou, M. de la Guardia, Early stage diagnosis of programmed cell death (apoptosis) using electroanalysis: nanomaterial and methods overview, TrAC, Trends Anal. Chem. 93 (2017) 199–211, 10.1016/j.trac.2017.06.007.
[11] A. Mugweru, B. Wang, J. Rusling, Voltammetric sensor for oxidized DNA using ultrathin films of osmium and ruthenium metallopolymers, Anal. Chem. 76 (2004) 5557–5563, 10.1021/ac049375j.
[12] M. Fojta, A. Danhel, L. Havran, V. Vyskočil, Recent progress in electrochemical sensors and assays for DNA damage and repair, TrAC, Trends Anal. Chem. 79 (2016) 160–167, 10.1016/j.trac.2015.11.018.
[13] M. Hasanzadeh, N. Shadjou, Pharmacogenomic study using bio- and nanobioelectrochemistry: drug–DNA interaction, Mater. Sci. Eng. C 61 (2016) 1002–1017, 10.1016/j.msec.2015.12.020.
[14] E. Paleček, M. Bartošík, Electrochemistry of nucleic acids, Chem. Rev. 112 (2012) 3427–3481, 10.1021/cr200303pp.

[15] I. Sanjuán, A. Martín-Gómez, J.P. Graham, N. Hernández-Ibáñez, C.E. Banks, T. Thiemann, J. Iniesta, The electrochemistry of 5-halocytosines at carbon based electrodes towards epigenetic sensing, Electrochim. Acta 282 (2018) 459–468, 10.1016/j.electacta.2018.06.050.
[16] E.E. Ferapontova, DNA electrochemistry and electrochemical sensor for nucleic acids, Annu. Rev. Anal. Chem. 11 (2018) 197–218, 10.1146/annurev-anchem-061417-125811.
[17] G.A. Evtugyn, A.V. Porfireva, S.V. Belyakova, Electrochemical DNA sensors for drug determination, J. Pharmaceut. Biomed. Anal. 221 (2022) 115058, 10.1016/j.jpba.2022.115058.
[18] A.M. Oliveira-Brett, V.C. Diculescu, T.A. Enache, I.P.G. Fernandes, A.-M. Chiorcea-Paquim, S.C.B. Oliveira, Bioelectrochemistry for sensing amino acids, peptides, proteins and DNA interactions, Curr. Opin. Electrochem. 14 (2019) 173–179, 10.1016/j.coelec.2019.03.008.
[19] L. Havran, J. Vacek, K. Cahová, M. Fojta, Sensitive voltammetric detection of DNA damage at carbon electrodes using DNA repair enzymes and an electroactive osmium marker, Anal. Bioanal. Chem. 391 (2008) 1751–1758, 10.1007/s00216-008-1850-1.
[20] Y. Zhang, H. Zhang, N. Hu, Using exonuclease III to enhance electrochemical detection of natural DNA damage in layered films, Biosens. Bioelectron. 23 (2008) 1077–1082, 10.1016/j.bios.2007.10.019.
[21] A.C. Papageorgiou, G.A. Posypanova, C.S. Andersson, N.N. Sokolov, J. Krasotkina, Structural and functional insights into Erwinia carotovora L-asparaginase, FEBS J. 275 (2008) 4306–4316, 10.1111/j.1742-4658.2008.06574.x.
[22] D.D. Zhdanov, V.S. Pokrovsky, M.V. Pokrovskaya, S.S. Alexandrova, M.A. Eldarov, D.V. Grishin, M.M. Basharov, Y.A. Gladilina, O.V. Podobed, N.N. Sokolov, Inhibition of telomerase activity and induction of apoptosis by Rhodospirillum rubrum L-asparaginase in cancer Jurkat cell line and normal human CD4+ T lymphocytes, Cancer Med. 6 (2017) 2697–2712, 10.1002/cam4.1218.
[23] Z. Darzynkiewicz, D. Galkowski, H. Zhao, Analysis of apoptosis by cytometry using TUNEL assay, Methods 44 (2008) 250–254, 10.1016/j.ymeth.2007.11.008.
[24] A.G. Ferrari, S.J. Rowley-Neale, C.E. Banks, Screen-printed electrodes: transitioning the laboratory in-to-the field, Talanta Open 3 (2021) 100032, 10.1016/j.talo.2021.100032.
[25] S. Manna, A. Sharma, A.K. Satpati, Electrochemical methods in understanding the redox processes of drugs and biomolecules and their sensing, Curr. Opin. Electrochem. 32 (2022) 100886, 10.1016/j.coelec.2021.100886.
[26] G. Paimard, E. Ghasali, M. Baeza, Screen-printed electrodes: fabrication, modification, and biosensing applications, Chemosensors 11 (2023) 113, 10.3390/chemosensors11020113.
[27] S. Carrara, C. Baj-Rossi, C. Boero, G.D. Micheli, Do carbon nanotubes contribute to electrochemical biosensing? Electrochim. Acta 128 (2014) 102–112, 10.1016/J.ELECTACTA.2013.12.123.
[28] V. Shumyantseva, T. Bulko, V. Pronina, S. Kanashenko, M. Pokrovskaya, S. Aleksandrova, D. Zhdanov, Electroenzymatic model system for the determination of catalytic activity of Erwinia carotovora L-asparaginase, Processes 10 (2022) 1313, 10.3390/pr10071313.
[29] L. Agafonova, D. Zhdanov, Y. Gladilina, S. Kanashenko, V. Shumyantseva, A pilot study on an electrochemical approach for assessing transient DNA transfection in eukaryotic cells, J. Electroanal. Chem. 920 (2022) 116635, 10.1016/j.jelechem.2022.116635.
[30] L. Agafonova, E. Tikhonova, M. Sanzhakov, L. Kostryukova, V. Shumyantseva, Electrochemical studies of the interaction of phospholipid nanoparticles with dsDNA, Processes 10 (2022) 2324, 10.3390/pr10112324.
[31] V.V. Shumyantseva, T.V. Bulko, L.E. Agafonova, V.V. Pronina, L.V. Kostryukova, Comparative analysis of the interaction between the antiviral drug umifenovir and umifenovir encapsulated in phospholipids micelles (Nanosome/Umifenovir) with dsDNA as a model for pharmacogenomic analysis by electrochemical methods, Processes 11 (2023) 922, 10.3390/pr11030922.
[32] L.V. Sigolaeva, T.V. Bulko, M.S. Kozin, W. Zhang, M. Köhler, I. Romanenko, J. Yuan, F.H. Schacher, D.V. Pergushov, V.V. Shumyantseva, Long-term stable poly (ionic liquid)/MWCNTs inks enable enhanced surface modification for electrooxidative detection and quantification of dsDNA, Polymer 168 (2019) 95–103, 10.1016/j.polymer.2019.02.005.
[33] L.V. Sigolaeva, T.V. Bulko, A.Yu Konyakhina, A.V. Kuzikov, R.A. Masamrekh, J.B. Max, M. Köhler, F.H. Schacher, D.V. Pergushov, V.V. Shumyantseva, Rational design of amphiphilic diblock copolymer/MWCNT surface modifiers and their application for direct electrochemical sensing of DNA, Polymers 12 (2020) 1514, 10.3390/polym12071514.
[34] V.V. Shumyantseva, T.V. Bulko, E.G. Tikhonova, M.A. Sanzhakov, A.V. Kuzikov, R.A. Masamrekh, D.V. Pergushov, F.H. Schacher, L.V. Sigolaeva, Electrochemical studies of the interaction of rifampicin and nanosome/rifampicin with dsDNA, Bioelectrochemistry 140 (2021) 107736, 10.1016/j.bioelechem.2020.107736.
[35] D. Janiszek, M.M. Karpińska, A. Niewiadomy, A. Kośmider, A. Girstun, H. Elzanowska, P.J. Kulesza, Differences in electrochemical response of prospective anticancer drugs IPBD and Cl-IPBD, doxorubicin and Vitamin C at plasmid modified glassy carbon, Bioelectrochemistry 137 (2021) 107682, 10.1016/j.bioelechem.2020.107682.
[36] D. Janiszek, M.M. Karpinska, A. Niewiadomy, A. Girstun, H. Elzanowska, M. Maj-Zurawska, P.J. Kulesza, Phase transition detection in accumulation of a potential anticancer drug Cl-ipbd with DNA: supercoiled and linear pUC19 plasmids, Electrochim. Acta 210 (2016) 422–434, 10.1016/j.electacta.2016.05.159.
[37] A.M. Oliveira-Brett, Electrochemical DNA assays, in: P.N. Bartlett (Ed.), Bioelectrochemistry: Fundamentals, Experimental Techniques and Applications, John Wiley & Sons, 2008, pp. 411–442, 10.1002/9780470753842.ch12.
[38] J. Ding, W. Qin, Potentiometric sensing of nuclease activities and oxidative damage of single-stranded DNA using a polycation-sensitive membrane electrode, Biosens. Bioelectron. 47 (2013) 559–565, 10.1016/j.bios.2013.03.066.
[39] D.D. Zhdanov, T. Fahmi, X. Wang, E.O. Apostolov, N.N. Sokolov, S. Javadov, A.G. Basnakian, Regulation of apoptotic endonucleases by EndoG, DNA Cell Biol. 34 (2015) 316–326, 10.1089/dna.2014.2772.
[40] D.D. Zhdanov, A.A. Plyasova, V.S. Pokrovsky, M.V. Pokrovskaya, S.S. Alexandrova, Y.A. Gladilina, N.N. Sokolov, Inhibition of nuclease activity by a splice-switching oligonucleotide targeting deoxyribonuclease 1 mRNA prevents apoptosis progression and prolong viability of normal human CD4+ T-lymphocytes, Biochimie 174 (2020) 34–43, 10.1016/j.biochi.2020.04.009.
[41] M.V. Pokrovskaya, V.S. Pokrovsky, S.S. Aleksandrova, N.N. Sokolov, D.D. Zhdanov, Molecular analysis of L-asparaginases for clarification of the mechanism of action and optimization of pharmacological functions, Pharmaceutics 14 (2022) 599, 10.3390/pharmaceutics14030599.